

# PCCP

Accepted Manuscript



This is an *Accepted Manuscript*, which has been through the Royal Society of Chemistry peer review process and has been accepted for publication.

*Accepted Manuscripts* are published online shortly after acceptance, before technical editing, formatting and proof reading. Using this free service, authors can make their results available to the community, in citable form, before we publish the edited article. We will replace this *Accepted Manuscript* with the edited and formatted *Advance Article* as soon as it is available.

You can find more information about *Accepted Manuscripts* in the [Information for Authors](#).

Please note that technical editing may introduce minor changes to the text and/or graphics, which may alter content. The journal's standard [Terms & Conditions](#) and the [Ethical guidelines](#) still apply. In no event shall the Royal Society of Chemistry be held responsible for any errors or omissions in this *Accepted Manuscript* or any consequences arising from the use of any information it contains.

**Study of photophysical properties of  
5-deazaalloxazine and 1,3-dimethyl-5-deazaalloxazine in  
dependence of pH using different spectral techniques<sup>†</sup>**

Dorota Prukała<sup>\*a</sup>, Mateusz Gierszewski<sup>a</sup>, Jerzy Karolczak<sup>b,c</sup> and Marek Sikorski<sup>a</sup>

<sup>a</sup> Faculty of Chemistry, Adam Mickiewicz University in Poznań, Umultowska 89b, 61-614 Poznań, Poland

<sup>b</sup> Faculty of Physics, Adam Mickiewicz University in Poznań, Umultowska 85, 61-614 Poznań, Poland

<sup>c</sup> Centre of Ultrafast Laser Spectroscopy, A. Mickiewicz University, Umultowska 85, 61-614 Poznań, Poland

Fax: +48 61 8291555, Tel: +48 61 8291593, dprukala@amu.edu.pl

**Abstract:**

The photophysical properties of 5-deazaalloxazine and 1,3-dimethyl-5-deazaalloxazine at different pH were characterized using absorption spectra, fluorescence emission spectra, fluorescence excitation spectra, synchronous fluorescence spectra and total fluorescence spectra. Their ionised and/or neutral forms were discussed in comparison with those obtained for other derivatives of 5-deazaalloxazine and/or 5-deaza<sup>iso</sup>alloxazine.

Steady-state and time-resolved techniques were used to study the protonation/deprotonation equilibria between cationic and neutral forms of both compounds and between neutral and monoanionic forms of 5-deazaalloxazine, as well as between monoanionic forms of this compound and its dianion. We estimated  $pK_a$  values for these equilibria both in the ground and excited states.

Our steady-state and time-resolved measurements indicate that cation of 5-deazaalloxazine in its isoalloxazinic form exhibits fluorescence that is quenched by protons in a dynamic process. Contrary to that, the cation of 1,3-dimethyl-5-deazaalloxazine has almost no fluorescence. Additionally, we found that the neutral forms of 5-deazaalloxazine and 1,3-methyl-5-deazaalloxazine are also quenched in acidic conditions by protons.

In basic conditions, 5-deazaalloxazine forms two structurally different anions, namely the alloxazinic monoanion and the isoalloxazinic monoanion; both simultaneously dissociate into the isoalloxazinic dianion at still higher pH.

The synchronous fluorescence spectra and total fluorescence spectra demonstrated their suitability to characterize and differentiate different fluorescent forms of 5-deazaalloxazine, namely: cation, neutral form, two monoanions, and dianion, in a wide pH range.

**Keywords:** 5-Deazaalloxazine, Acid-base equilibria, Absorbance, Steady-state fluorescence, Synchronous fluorescence spectra, 3D spectra, Time-resolved fluorescence.



We dedicate this paper to the memory of Prof. Jacek Koziol.

## Introduction

5-Deazaalloxazine (pyrimido[4,5-*b*]quinoline-2,4(1*H*,3*H*)-dione) is homologous of 5-deazaflavins (pyrimido[4,5-*b*]quinoline-2,4(3*H*,10*H*)-diones), compounds that are cofactors for flavin-dependent enzymatic reactions.<sup>1</sup> 5-Deazaflavin shaped coenzyme was also found in methane producing bacteria.<sup>2</sup>

Such compounds have their own redox system different from that of the well known riboflavin<sup>1</sup> and play a significant role in the redox reactions occurring in biological systems.<sup>3,4</sup> Some derivatives of 5-deazaflavin and its analogs with 5-deazaalloxazine structure were reported as showing antitumor activity *in vitro*,<sup>5-9</sup> they show antimalarial, antibacterial, analgesic and antitumor activities.<sup>8,10</sup>

5-Deazaalloxazines has also been studied because their alloxazine scaffold undergoes photoinduced tautomerization in the presence of acetic acid, changing its alloxazinic emission into “isoalloxazine” emission.<sup>11,12</sup> Such behavior is similar to that of alloxazines (derivatives of flavins) which also undergo excited state double proton transfer, catalyzed by carboxylic acids, such as acetic acid, and other organic compounds.<sup>13-15</sup>

These two classes of compounds possess similar structures, with certain similarity in their spectral, photophysical and photochemical properties.<sup>1,16</sup>

**Figure 1** presents the structures and atom numbering of the studied compounds, and the structure of a simple alloxazine for comparison.

Insert Figure 1

On the basis of our recent work, we conclude that the behaviour of an alloxazine derivative (lumichrome)<sup>17</sup> is similar to that of 5-deazaalloxazine (9-methyl-5-deazaalloxazine)<sup>18</sup> in aqueous solutions at different pH; however, the values of the absorption and emission maxima of the corresponding species (cationic, neutral and anionic forms) of these compounds are shifted relative to each other. The acid-base properties of alloxazines (mainly lumichromes)

69 have been studied quite intensively,<sup>17,19-21</sup> while less information is available on the acid-base  
70 equilibria of the derivatives of 5-deazalloxazine.<sup>18</sup>

71 According to our previous work<sup>17</sup>, lumichrome (7,8-dimethylalloxazine) exists as neutral  
72 form in the 1 to 8 pH range, similarly to 9-methyl-5-deazalloxazine, which exists in its neutral  
73 form in the pH range from 1.2 to about 9.<sup>18</sup> Next, at still higher pH, these compounds undergo  
74 deprotonation in a similar way. Namely, they dissociate their both hydrogen atoms from N(1)  
75 and N(3) positions in the same pH range, forming two monoanions. The N(1) monoanion has  
76 isoalloxazinic form and the N(3) monoanion has alloxazinic form, for both compounds.  
77 Additionally, the  $pK_a$  values for the reaction leading to the formation of monoanions in the  
78 ground state are similar to that in the excited state. Also at high pH values (12 - 14) the  
79 isoalloxazinic dianion is formed for both compounds.

80 In the present work we explore spectral and photophysical properties of 5-deazaalloxazine (5-  
81 DAll) and 1,3-dimethyl-5-deazaalloxazine (1,3Me-5-DAll), at different pH conditions, with a  
82 special attention to their cationic forms. We use the traditional absorption, fluorescence and  
83 fluorescence excitation spectra, together with fluorescence lifetime measurements and some  
84 additional spectral methods - three-dimensional fluorescence spectra (3D), for the fingerprint  
85 analysis of different neutral and ionic forms of 5-deazaalloxazine. We also present the  
86 fluorescence synchronous spectra, which are used to better distinguish and identify the  
87 fluorescent species (i.e. protonated and neutral forms, monoanions, and dianions) present in  
88 aqueous solutions of the investigated 5-deazaalloxazines at different pH.

89

## 90 **Experimental**

91 5-DAll and 1,3Me-5-DAll were available from previous work.<sup>12</sup> Hydrochloric acid and  
92 sodium hydroxide were from Aldrich. Water was triply distilled. We performed titration  
93 experiments three times, including preliminary measurements. During the second and the  
94 third measurements we paid particular attention to the inflection points. At first, weighed

amounts of 5-DAll or 1,3Me-5-DAll were dissolved in 10 mL of 2 M HCl. Next, an appropriate volume of 2 M NaOH was added resulting in  $\text{pH} \approx 7$ . These solutions were titrated with 2 M or 4 M NaOH (HCl) to the appropriate pH values. The exact pH of each solution was determined using a Hanna Instruments pH-meter. Samples of high acidity were prepared by dissolving weighed amounts of 5-DAll or 1,3Me-5-DAll in more concentrated HCl solutions. We maintained the same concentration of the titrated alloxazine in each solution. Alternatively, the spectra measured for very high and very low pH values were corrected for the sample concentration. The pH values are indicated in the respective Figures. The absorption and emission spectra were collected for all of the pH points. The remaining spectra were measured only for the selected pH values.

All solutions were prepared on the same day as their spectra were recorded. The time-resolved fluorescence measurements were also performed at the same time, in order to minimize any photolytic or hydrolysis reactions.

UV-Vis absorption spectra were recorded on a Jasco V-650 spectrophotometer. Emission, excitation and 3D (three-dimensional) fluorescence spectra were recorded on a Horiba Jobin-Yvon-Spex Fluorolog 3-22 spectrofluorometer. Right-angle geometry was used for all steady state emission measurements. Fluorescence spectra were collected with 1 nm excitation and emission slits, and 0.3 s integration time. For the 3D fluorescence spectra, excitation and emission slits were 1 nm; the acquisition interval was 2 nm and the integration time was 0.1 s. 3D emission spectra were collected between 350 to 650 nm in the 290-500 nm range of the excitation wavelengths, spaced by 5 nm intervals in the excitation domain.

Fluorescence lifetime measurements of 5-DAll and 1,3Me-5-DAll were performed using the time-correlated single-photon counting (TCSPC) method. Decays were measured with the TCSPC Triple Illuminator as an accessory for the Fluorolog<sup>®</sup> 3-22 steady-state spectrofluorometer that adds lifetime-capability in the time domain. The excitation source was

a NanoLED diode ( $\lambda_{\text{exc}}=338$  nm or 368 nm, fwhm  $\approx$  250 ps) from IBH. The instrument in this hardware configuration is capable of measuring lifetimes as short as 400 ps. Deconvolution of the fluorescence decay curves was performed using IBH Consultants software. All of the experiments were carried out at room temperature (298 K).

Fluorescence lifetime measurements for the samples of high acidity were performed at the Centre for Ultrafast Laser Spectroscopy in Poznań, with the respective fluorescence lifetime spectrophotometer setup, using single-photon timing technique, described in detail elsewhere.<sup>22</sup> The samples were excited at  $\lambda_{\text{exc}}=375$  nm and the emissions were observed at 420 nm and 500 nm. A Spectra-Physics pico/femtosecond laser system was used as the source of exciting pulses. That included a Tsunami Ti: sapphire laser, pumped with a BeamLok 2060 argon ion laser, which generated 1-2 ps pulses at a repetition rate of about 82 MHz and average power of over 1 W, tuneable in the 720-1000 nm range. The repetition rate of the excitation pulses was variable from 4 MHz to single-shot by using a model 3980-2S pulse selector. Second and third harmonics of the picosecond pulse obtained on a GWU-23PS harmonic generator could be used for excitation, giving great flexibility in the choice of the excitation wavelength. Elements of an Edinburgh Instruments FL900 system were used in the optical and control components of the system. The pulse timing and data processing systems employed a biased TAC model TC 864 (Tenelec) and the R3809U-05 MCP-PMT emission detector with thermoelectric cooling and appropriate preamplifiers (Hamamatsu).

## Results and discussion

### *Ground and excited state equilibria between cationic and neutral forms of 5-deazaalloxazine and 1,3-dimethyl-5-deazaalloxazine*

Absorption spectra of 5-DAll and 1,3Me-5-DAll in acidic conditions up to pH 5 are presented in **Figure 2**, respectively in panels A and B. Absorption bands of both protonated and neutral

molecules of the two compounds are detected in this pH range. The 5-DAll cations (**C5D<sup>+</sup>**, see **Figure 3**) and 1,3Me-5-DAll cations (**CMe5D<sup>+</sup>**, see **Figure 3**) have absorption bands with a single maximum, at 331 nm for the first compound and 332 nm for the second. The molar absorption coefficients, measured at band maxima, are  $\epsilon = 14400 \text{ dm}^3\text{mol}^{-1}\text{cm}^{-1}$  for 5-DAll and  $\epsilon = 7800 \text{ dm}^3\text{mol}^{-1}\text{cm}^{-1}$  for 1,3Me-5-DAll, as it is presented in Table 1.

Insert Figure 2.

At higher pH, 5-DAll and 1,3Me-5-DAll exist as the respective neutral forms, labeled **N5D** and **NMe5D** (see **Figure 3**). Theirs absorption spectra show characteristic alloxazinic-type bands with two maxima in the lowest-energy range.

For 5-DAll, the first maximum is situated at  $\lambda_1 = 354 \text{ nm}$  ( $\epsilon = 4300 \text{ dm}^3\text{mol}^{-1}\text{cm}^{-1}$ ) and the second at  $\lambda_2 = 312 \text{ nm}$  ( $\epsilon = 8500 \text{ dm}^3\text{mol}^{-1}\text{cm}^{-1}$ , Table 1). The maxima of 1,3Me-5-DAll are situated at  $\lambda_1 = 357 \text{ nm}$  ( $\epsilon = 3600 \text{ dm}^3\text{mol}^{-1}\text{cm}^{-1}$ ), and at  $\lambda_2 = 312 \text{ nm}$  ( $\epsilon = 6500 \text{ dm}^3\text{mol}^{-1}\text{cm}^{-1}$ , Table 1). Someone can note effect of decrease of molar absorption coefficients, associated with the presence of methyl groups in 1,3Me-5-DAll comparing its  $\epsilon$  to respective values recorded for 5-DAll.

Insert Table 1

According to these spectra, we calculated the acid-base equilibria between protonated and neutral forms, as shown in **Figure 3**. Note that we attributed alloxazinic structures to the 5-DAll cation (**C5D<sup>+</sup>** form, and not **C5ID<sup>+</sup>**, which has been detected in the excited state, see the discussion below) and the 1,3Me-5-DAll cation (**CMe5D<sup>+</sup>** form, and not **CMe5ID<sup>+</sup>**, see the discussion below) existing in the ground state.

Insert Figure 3

We used the DATAN software package in the total titration experiment<sup>23</sup> to calculate the  $\text{pK}_a$  values for all equilibria between the individual species of 5-DAll and 1,3Me-5-DAll.

The estimated value of  $pK_{a1} = 0.7$  for 5-DAll reflects the equilibrium between **N5D** and **C5D**<sup>+</sup> forms in the ground state. The  $pK_{a1} = 0.3$ , was found for the equilibrium between **NMe5D** and **CMe5D**<sup>+</sup> forms of 1,3Me-5-DAll.

The emission spectra of 5-DAll ( $\lambda_{exc} = 310$  nm) and 1,3Me-5-DAll ( $\lambda_{exc} = 320$  nm) for the solutions of high acidity are presented in **Figure 2** (panels C and D, respectively).

The emission spectra of 5-DAll (**Figure 2**, panel C) in acidic conditions show two emissions bands. At  $pH < 0.3$ , there is one emission band with the maximum at 461 nm, which we attribute to the emission of the protonated form of 5-DAll. It is the first time when the emission of the 5-DAll cation is presented. Additionally, the intensity of this emission band decreases at lower pH. This is the effect of quenching of the cationic form of 5-DAll, caused by the protons  $H^+$ , as we shall explain in more detail below.

We believe that the 5-DAll cation has an isoalloxazinic form (**C5ID**<sup>+</sup> in **Figure 3**), because its emission is typically red-shifted, as compared to that of the alloxazinic form, with the emission band maximum coincident with that of 10-ethyl-5-deaza*iso*alloxazine.<sup>18</sup>

At higher pH value ( $pH > 2.5$ ), 5-DAll shows typical alloxazinic - type emission, which belongs to the **N5D** neutral form (**Figure 3**) with the maximum at 423 nm.

The fluorescence excitation spectra observed at  $\lambda_{em}$  460 nm (see **Figure 2**, panel E), measured for 5-DAll in acidic pH, overlap the absorption spectra very well.

The emission spectra of 1,3Me-5-DAll in acidic conditions presented in **Figure 2D** show only one band with its maximum at 421 nm. The intensity of this band strongly increases with increasing pH value. We attribute this band to the emission of the neutral form of 1,3Me-5-DAll (**NMe5D** form, **Figure 3**). However, the decreasing fluorescence intensity of **NMe5D** at lower pH is also due to its quenching caused by protons ( $H^+$ ), as we shall detail below.



This emissive neutral form of 1,3Me-5-DAll also exists at higher pH values, as can be observed in the same **Figure 2D** at pH 7.18 and pH 10.95. It is not surprising, considering that the 1,3Me-5-DAll molecule has no labile protons that can dissociate in basic solutions.

Based on our measurements, we conclude that the protonated form of 1,3Me-5-DAll has almost no fluorescence. Accordingly, the fluorescence excitation spectra presented in **Figure 2F** indicate that the emission comes mostly from the neutral form.

The  $pK_a^*$  values of 5-DAll and 1,3Me-5-DAll in their excited states determined using the DATAN software package in the total titration experiment give values  $pK_{a1}^* = 1.4$  for the equilibrium between the protonated and neutral forms of 5-DAll, and  $pK_{a1}^* = 1.0$  for the equilibrium between the protonated and neutral forms of 1,3Me-5-DAll (**Figure 3**). However, these values are valid as the estimates only, due to interference of the already mentioned quenching.

Table 1 collects also the fluorescence quantum yields of 5-DAll and 1,3Me-5-DAll in acidic, neutral, and basic aqueous solutions. These data were obtained by excitation of the solutions at  $\lambda_{exc} = 320$  nm and also at  $\lambda_{exc} = 410$  nm, when it is possible.

The fluorescence quantum yield of 5-DAll is low in strong acidic condition. For example, it is  $\phi = 0.02$ , when  $-\log [H^+] = -0.48$ . This is the region where mostly the cationic form of 5-DAll (**CMe5D<sup>+</sup>**) exists. The fluorescence quantum yield grows simultaneously with rising of pH value. At pH 2.5, where the neutral form of 5-DAll (**N5D**) becomes predominant, the fluorescence quantum yield is  $\phi = 0.18$ . This neutral form of 5-DAll exist solely in the solution up to about pH = 7, where its fluorescence quantum yield achieves value of  $\phi = 0.21$ .

It is the fluorescence quantum yield of non-quenched **N5D** form of 5-DAll. The fluorescence of 1,3Me-5-DAll is due only to the neutral form of this compound (**NMe5D**) because, as we mentioned above, its cationic form (**CMe5D<sup>+</sup>**) has almost no fluorescence. The fluorescence quantum yield of **NMe5D** is  $\phi = 0.19$ . This value was obtained for neutral and basic solutions

of 1,3Me-5-DAll. But in acidic solutions the fluorescence of **NMe5D** is lower, because this form is quenched by protons (see Table 1).

*Ground and excited state equilibria between neutral and anionic forms of 5-deazaalloxazine*

**Figure 4** shows the absorption (panel A) and emission spectra (panel B,  $\lambda_{\text{ex}} = 320$  nm) of 5-DAll in the pH range from 6.02 to 11.27. There is almost no effect of pH on the alloxazinic-type absorption maxima of the studied compound in this pH range. At higher pH values, the longer-wavelength maximum is slightly red-shifted from that corresponding to the neutral form at  $\lambda = 351$  nm to that of the alloxazinic-type monoanion at  $\lambda = 358$  nm ( $\epsilon = 8600$  dm<sup>3</sup>mol<sup>-1</sup>cm<sup>-1</sup>, Table 1). There is also a new band, appearing at higher pH. We compared this band, peaking at about  $\lambda = 380$  nm ( $\epsilon = 3900$  dm<sup>3</sup>mol<sup>-1</sup>cm<sup>-1</sup>, Table 1) to the lowest-energy band of 10-ethyl-5-deza $\textit{iso}$ alloxazine with its maximum at 389 nm<sup>18</sup>, concluding that this band has  $\textit{iso}$ alloxazinic structure. Molar absorption coefficients for monoanions were calculated using deconvoluted absorption spectra of 5-DAll at pH 10.16, assuming that the concentrations of both monoanions are the same.

Insert Figure 4

Based on these spectra and our earlier works<sup>17,18</sup>, we conclude that the two different 5-DAll monoanions are formed almost simultaneously in this pH range (see **Figure 5**). One of these has alloxazinic structure, while the second has  $\textit{iso}$ alloxazinic structure. We ascribed the  $\textit{iso}$ alloxazinic structure to the second monoanion on the basis of the position of its absorption and emission bands, which are red-shifted as compared to the alloxazinic bands, being similar to the absorption and emission bands of 10-ethyl-5-deza $\textit{iso}$ alloxazine.<sup>18</sup> The  $\textit{iso}$ alloxazinic monoanion can only be formed by the abstraction of hydrogen from the N(1)-H group, although we conclude that it has the **ID1** structure. The structures **AD1** and **ID1** seem to be the only resonance structures, although we believe they are not equivalent, with the

(isoalloxazinic) **ID1** form contributing substantially to the resonance hybrid of this monoanion. The same reasoning applies to **C5D<sup>+</sup>** and **C5ID<sup>+</sup>** forms (**Figure 3**), and the **ID13** form (**Figure 5**). We can also compare the anionic structures of 5-DAll to the anionic structures of lumichrome (7,8-dimethylalloxazine) derivatives, having similar properties in basic media. Our calculations by means of the density-functional theory (DFT) suggested that the monoanion formed by hydrogen abstractions from the N(1) position of lumichrome may exist in the isoalloxazinic form, with a large contribution of the negative charge on the N(10) atom.<sup>17</sup> Note that the N(3) monoanion has no alternatives other than forming the alloxazinic-type structure (**AD3**).

Insert Figure 5

Based on the absorption spectra, we calculated the  $pK_{a2}$  and  $pK_{a3}$  values in the ground state for the equilibria between the **N5D** form and the two monoanions (**ID1** and **AD3** forms), obtaining  $pK_{a2} = pK_{a3} = 8.9$  (**Figure 5**).

We also studied the equilibria between the neutral molecule and the two monoanions of 5-DAll in the excited state.

Excitation at 320 nm of 5-DAll solution at pH = 7.24 gives the emission band with the maximum at  $\lambda = 422$  nm (**Figure 4B**), still corresponding to the neutral form. Two new bands appeared at higher pH, one peaking at  $\lambda = 410$  nm and the second broad band with the maximum at  $\lambda = 480$  nm, appearing as a shoulder in **Figure 4B**. We attribute these new bands to the two monoanions of 5-DAll (**ID1** and **AD3**, **Figure 6**). In particular, the hypsochromically shifted emission band is attributed to the alloxazinic monoanion (**AD3**) and the bathochromically shifted emission band to the isoalloxazinic monoanion (**ID1**), by comparison to other similar substances.<sup>18</sup>

According to our measurements, the  $pK_a^*$  values in the excited state are quite similar to those in the ground state. The calculated values for 5-DAll obtained from the emission spectra

yielded  $pK_{a2}^* = pK_{a3}^* = 9.0$  for the equilibria between the neutral and the two deprotonated monoanions (**ID1** and **AD3**, **Figure 5**). Thus, the dissociation in the excited state occurs both at N(1)-H and N(3)-H in the same pH range.

The fluorescence excitation spectra of a solution of target compound at pH range from 7.2 to 11.3 (**Figure 4C**), observed at 420 nm, reproduces the absorption bands with the maxima at about 350 nm and 312 nm. The emission at 420 nm originates mostly from the alloxazinic forms of 5-DAll, including the neutral molecule (**N5D**) in lower pH, and the monoanion (**AD3**) in higher pH. Note that the latter emission band is slightly hipsochromically shifted (**Figure 4B**). There are no neutral molecules of 5-DAll at pH > 10, as could be deduced from the  $pK_{a2}^*$  value calculated above. Thus, we assume that at higher pH the alloxazinic - type emission comes from the monoanion, existing in the ground state. The existence of the alloxazinic-type monoanion in the ground state would not be so obvious on the basis of absorption spectra alone, because the spectra of the neutral form and the alloxazinic monoanion are very similar.

However, the excitation spectra of the emission detected at 460 nm and 500 nm (**Figure 4**, panel D) reproduce the most bathochromically shifted part in the absorption spectra (**Figure 4**, panel A; all spectra except the one at pH 7.2). This indicates that the isoalloxazinic monoanion (**ID1**) also exists in the ground state.

**Figure 6** (panel A) shows the absorption spectra of 5-DAll at the 11.27 - 13.57 pH range. Note that the alloxazinic - type absorption disappears while the isoalloxazinic - type absorption grows at higher pH values. Therefore, we conclude that the 5-DAll dianion exists in the isoalloxazinic **ID13** form, with its absorption peaking at  $\lambda = 391$  nm. The molecular absorption coefficient for this dianion is  $\epsilon = 5400 \text{ dm}^3 \text{ mol}^{-1} \text{ cm}^{-1}$ .

Insert Figure 6

The estimated  $pK_{a4} = pK_{a5} = 13.0$  reflect the equilibrium constant for the formation of the **ID13** dianion in the ground state, from both the **ID1** and **AD3** monoanions.

The emission spectra of the **ID13** dianion existing at pH 13 to 13.57 show a single distinct band with its maximum at 481 nm (**Figure 6**, panel B). Note that the maxima of the emission bands of the isoalloxazinic **ID1** monoanion and the **ID13** dianion are very similar. They differ only by the intensities of the bands.

The fluorescence excitation spectra recorded using 420 nm emission, confirm that the emission from the alloxazinic monoanion disappears at higher pH (see **Figure 6**, panel C). Additionally the fluorescence excitation spectra observed at 500 nm indicate that the emission in the 11.62 – 13.57 pH range comes from different species, namely from the **ID1** monoanion and the **ID13** dianion, as evidenced by the bathochromically shifted excitation spectra of **ID13** as compared to the spectra of **ID1**.

The equilibrium constant for the formation of the **ID13** dianion in the excited state is slightly lower:  $pK_{a4}^* = pK_{a5}^* = 12.6$ , according to the results obtained using the DATAN software package.

The fluorescence quantum yields of 5-DAll monoanions are lower than the fluorescence quantum yield of neutral form of this compound (see Table 1). Both these monoanions predominate in the solution at 8 – 12 pH range. It is difficult to estimate the fluorescence quantum yield of alloxazinic monoanion (**AD3**) because its absorption and fluorescence spectra always overlap the spectra of isoalloxazinic monoanion (**ID1**). However, when we use  $\lambda_{exc} = 320$  nm for excitation, we excite mainly **AD3** monoanion with a small contribution of **ID1** form. For such conditions, calculated value of fluorescence quantum yield  $\phi = 0.07$  we can attribute mainly to **AD3** form. But when we use  $\lambda_{exc} = 410$  nm, the only isoalloxazinic **ID1** monoanion is excited. So the fluorescence quantum yields  $\phi = 0.16$  we attributed to the isoalloxazinic monoanion of 5-DAll. The fluorescence quantum yield of **ID13** dianion is  $\phi =$

0.19. This value is calculated for strong, basic solutions of 5-DAll (pH > 12.5), because in such conditions **ID13** dianion exists as the only form.

### *Synchronous fluorescence spectra of 5-DAll and 1,3Me-5-DAll in aqueous solution of different pH*

We registered synchronous fluorescence spectra (SFS) for both compounds. These spectra are used for finding the number of emitting species existing in solution, and is widely used in biological, environmental, and clinical application.<sup>24</sup>

We expected that SFS would produce better-resolved single bands for each of the species, namely cationic, neutral and anionic forms of the investigated compounds, with the results corresponding to those obtained from conventional fluorescence measurements.

According to our best knowledge this method has not been used for analysis of equilibria of different forms of target compound, existing at different pH.

**Figure 7** presents raw SFS in different pH ranges.

Insert Figure 7

The synchronous fluorescence intensity can be described as follows:<sup>25</sup>

$$I_s = Kcb \text{Ex}(\lambda_{\text{exc}}) \text{Em}(\lambda_{\text{exc}} + \Delta\lambda)$$

Here,  $I_s$  is the synchronous fluorescence intensity;  $c$  – the concentration of the sample,  $\text{Ex}$  – the intensity of the excitation spectrum at  $\lambda_{\text{exc}}$ ,  $\text{Em}$  – the intensity of the emission spectrum at  $\lambda_{\text{exc}} + \Delta\lambda$ ,  $b$  the thickness of the sample; and  $K$  the constant describing the instrumental factors, including geometry and other parameters. Therefore, a synchronous fluorescence spectrum is a function of both the emission and the excitation spectrum of the compound or compounds of interest. SFS can be plotted as a function of wavelength of excitation ( $\lambda_{\text{exc}}$ ) or wavelengths of emission ( $\lambda_{\text{exc}} + \Delta\lambda$ ) used in recording it. We are presenting our SFS as a function of the emission wavelength.

The selected value of  $\Delta\lambda$  (offset) has a significant impact on the nature, maximum, and shape of the spectrum recorded. There is no general rule for choosing  $\Delta\lambda$ ; however, the bandwidth increases with  $\Delta\lambda$ . Additionally, the maxima of the SFS bands shift to the longer wavelengths with increasing  $\Delta\lambda$ . A simple rule is to use small values, 10 or 20 nm (the slit widths should be not exceed half of  $\Delta\lambda$ ) for species with a small Stokes shift, and larger values for compounds with larger Stokes shift.

As we can see in **Figure 7A**, the bands with their maxima at 394 nm with growing intensity, may be attributed to neutral 5-DAll in its alloxazinic form, because it appears also at higher pH. At lower pH we observe only a very small contribution of the cation (**C5ID**<sup>+</sup> form) because we used  $\Delta\lambda = 20$  nm, what is sufficient to observe the neutral form having small Stoke's shift, but is insufficient to observe the cationic form, which has a larger Stoke's shift. The spectra in **Figure 7B**, registered using  $\Delta\lambda = 60$  nm, show both the SFS band of the neutral form with its maximum red-shifted as compared to the previous spectrum ( $\lambda_{\text{max}} = 411$  nm) and the SFS band of **C5ID**<sup>+</sup> in its isoalloxazinic form, characterized by its maximum at  $\lambda_{\text{max}} = 431$  nm, appearing at low pH values.

**Figure 7C** shows the raw synchronous fluorescence spectra of 5-DAll appearing at 7.24 – 11.27 pH range, and **Figure 7D** shows SFS bands of 5-DAll at 11.62 – 13.57 pH range. These spectra were registered using  $\Delta\lambda = 20$  nm, with two separate bands apparent. The intensity of the first synchronous band in **Figure 7C** grows and shifts to the blue at higher pH. At pH about 11 this band has the maximum at 391 nm. We attribute this band to the monoanion with the **AD3** structure.

Thus, we were unable to obtain separate bands of the neutral form of 5-DAll and its alloxazinic monoanion. However, the maximum of the SFS band of the neutral form is at 394 nm, while the maximum of the SFS band of the alloxazinic monoanion is at 391 nm.

Simultaneously a new band appears with its maximum at 439 nm. We identify this low-intensity component as the **ID1** isoalloxazinic monoanion. Note that the total concentration of 5-DAll is kept the same in the entire 7.2 to 11.3 pH range, thus the growing synchronous bands at higher pH come from new emitting species. Generally the SFS of 5-DAll indicate that both monoanions appear in the same pH range.

The band attributed to the **AD3** monoanion disappears in the 11.62 to 13.57 pH range. A single band with the maximum at 444 nm remains at  $\text{pH} \geq 13.4$  (green bolded line in **Figure 7D**). Thus, the isoalloxazinic SFS band shifts to the red, and is attributed to the newly emerging **ID13** dianion of 5-DAll.

Insert Figure 8

**Figure 8** shows the raw synchronous fluorescence spectra of 1,3Me-5-DAll. There is only one SFS band of this compound in all solutions at different pH. This band with the maximum at 396 nm is attributed to the neutral form of 1,3Me-5-DAll. The intensity growth of this band is interpreted as resulting from the growing concentration of the **NMe5D** neutral form of 1,3Me-5-DAll, also taking into account the quenching of **NMe5D** occurring at low pH. The intensity of the SFS band remains constant at higher pH. There is no SFS band of the cationic form of 1,3Me-5-DAll, because, as we already discussed above, the cationic form of this compound exhibits no fluorescence.

#### ***Total fluorescence spectra of 5-DAll and 1,3Me-5-DAll at different pH***

The total fluorescence spectra of 5-DAll in strongly acidic solution are presented in **Figure 9A** and at  $\text{pH} = 13.57$  in **Figure 9H**. The total fluorescence is showed as a three-dimensional spectrum where x-axis represents the emission wavelengths, y-axis the excitation wavelengths and z-axis the fluorescence intensity. More total fluorescence spectra of 5-DAll at selected pH



values are shown as contour maps of the excitation-emission matrices (**Figure 9B - 9G**). Contour maps were plotted by linking points of equal fluorescence intensity.

Insert Figure 9

Using this method, we can perfectly trace the changes in total fluorescence of 5-DAll throughout the entire pH range. **Figures 9A and 9B** reveal an intensive band of the **C5ID<sup>+</sup>** cationic form of 5-DAll with the excitation at about 300 – 350 nm and the emission at about 425 – 550 nm.

**Figure 9C** shows the contour map of the total fluorescence of the 5-DAll neutral form, with the excitation at about 300 – 350 nm and emission at about 380 – 520 nm. This band is quite intensive, revealing two maxima on the excitation side and one – on the emission side. 5-DAll exists in equilibrium between the neutral form and the two monoanions at pH 9.1 (**ID1** and **AD3**, see **Figure 9D**). Note the bathochromically expanding bands, both on the excitation and the emission side. Only the two monoanions, **ID1** and **AD3**, remain in solution at pH 11.62 (**Figure 9E**). The bands of these two monoanions strongly overlap, but still there is a large area occupied by their total fluorescence spectra. This area ranges up to 450 nm on the excitation side and up to ca. 580 nm on the emission side. The band of the alloxazinic monoanion is shifted hipsochromically with the excitation at 300 - 380 nm and the emission at 400-450 nm, compared to the isoalloxazinic monoanion with a bathochromically shifted band. Going to pH = 12.51 (**Figure 19F**) the alloxazinic monoanion band disappears, accompanied by a further shift of the isoalloxazinic band to longer wavelengths on the emission side. This is interpreted as resulting from the formation of the 5-DAll dianion in its isoalloxazinic form (**ID13**). **Figures 9G and 9H** present the total fluorescence spectrum and its contour map of the pure **ID13** dianion. This band is observed with the excitation at about 300 - 450 nm and emission at about 420 - 620 nm.

#### *Time-resolved fluorescence measurements of 5-DAll and 1,3Me-5-DAll at selected pH*

The measured fluorescence lifetimes of 5-DAll in acidic conditions are presented in **Figure 10**. These measurements used the pico/femtosecond laser system, allowing to resolve very short lifetimes ( $\lambda_{\text{exc}} = 375$  nm). At higher pH (pH 1 – 3) the data were also supplemented with measurements using a NanoLED diode as an excitation source ( $\lambda_{\text{exc}} = 338$  nm and  $\lambda_{\text{exc}} = 368$  nm). In each case the goodness of fit was evaluated using reduced chi-square,  $\chi^2$ , Durbin-Watson, and ordinary-runs tests, as well as by visual inspection of the distribution of the weighted residuals and of the autocorrelation functions. **Figure 10A** shows the plot of the lifetimes vs.  $-\log [\text{H}^+]$  using 375 nm excitation and observing the emission at 420 nm, while **Figure 10B** presents measured lifetimes using 375 nm excitation and observing the emission at 500 nm. The numbers placed in the Figures indicate the percentage contribution of each of the emitting species.

Insert Figure 10

According to **Figure 2B**, the emission at 420 nm corresponds mainly to the alloxazinic form, while that at about 500 nm corresponds mainly to the isoalloxazinic form.

Note that in **Figure 10A**, we obtained single-exponential, double-exponential and triple-exponential decays, corresponding to the cationic and neutral forms of 5-DAll. On the other hand, we can see mainly single-exponential decays in **Figure 10B**. Additionally, the lifetimes of the fluorescent species decrease with the growing acidity. We conclude that the longer-living component with the lifetimes from 280 to 4700 ps corresponds to the **C5ID<sup>+</sup>** isoalloxazinic cation, being quenched by protons. The lifetimes of this cation at different pH are shown by red squares in **Figures 10A** and **10B**. A shorter-living component, appearing only in **Figure 10A**, is probably the **C5D<sup>+</sup>** alloxazinic cation of 5-DAll, indicated by black circles (The plot of the lifetimes of this cation vs.  $-\log [\text{H}^+]$  is given in **Figure 4s** in the Supporting Information). We come to this conclusion because this component is not

observable at higher pH values, being also absent if the emission is observed at longer wavelengths. The lifetime of this cation is growing from 9 ps to 20 ps with decreasing acidity. Blue triangles indicate lifetimes of the **N5D** neutral form of 5-DAll. As apparent in **Figure 10A**, this form is also quenched in solutions of higher acidity.

The results of kinetic study of fluorescence quenching of the **C5ID**<sup>+</sup> cation of 5-DAll in aqueous solutions in function of H<sup>+</sup> concentration is showed in **Figure 1s** in the Supporting Information. We used Stern-Volmer equations as follows:

$$I_0/I = 1 + k_q \times \tau_{F0} \times [H^+]$$

$$\tau_{F0}/\tau_F = 1 + k_q \times \tau_{F0} \times [H^+]$$

and the Stern-Volmer relation:

$$k_q \times \tau_{F0} = K_{SV}$$

Where:  $I_0$  - fluorescence intensity yield in absence of a quencher;  $I$  - fluorescence intensity in presence of a quencher;  $k_q$  - quenching rate constant;  $\tau_{F0}$  - fluorescence lifetime in absence of a quencher;  $\tau_F$  - fluorescence lifetime in presence of a quencher;  $[H^+]$  - quencher concentration;  $K_{SV}$  - Stern-Volmer constant.

The obtained values of the Stern-Volmer constant in the steady-state measurements is  $K_{SV1} = 1.53 \pm 0.15$ ; while the value obtained in the time-resolved study is  $K_{SV2} = 1.51 \pm 0.08$ .

The value of the quenching rate constant for the steady-state results is  $k_q = (3.25 \pm 0.16) \times 10^8 \text{ s}^{-1}$ ; while that for the time-resolved results  $k_q = (3.22 \pm 0.16) \times 10^8 \text{ s}^{-1}$ . Thus, the values obtained using these two methods are in a good agreement. The quenching of **C5ID**<sup>+</sup> in the experimental conditions is controlled by diffusion and has dynamic character. The **N5D** neutral form is also quenched by protons, as shown on **Figure 2s** (Supporting Information).

The Stern-Volmer constant in the time-resolved study is  $K_{SV3} = 22.57 \pm 0.08$ , while the value of the quenching rate constant  $k_q = (2.51 \pm 0.06) \times 10^9 \text{ s}^{-1}$ . Because the dependence of  $I_0/I$  on  $[H^+]$  is nonlinear, we conclude that the quenching operates by both static and dynamic

mechanisms. Indeed, the neutral and cationic forms of 5-DAll exist in the ground state, being involved in acid-base equilibria and the increasing of fluorescence intensity at higher pH is due mostly to the increasing of the neutral form concentration in the mixture.

Measuring the fluorescence decay at pH 2 – 14 (using NanoLED diode as a source,  $\lambda_{\text{exc}} = 368$  nm), the emission at 420 nm gave either a mono-exponential or a bi-exponential decay, depending on pH (see **Figure 11A**). Note that mainly the alloxazinic forms emit at this wavelength (see **Figure 2**, **Figure 4** and **Figure 6**).

Insert Figure 11

The longer-living component with about 9 ns lifetime corresponds to the neutral form of 5-DAll (**N5D**), while and shorter-living component with about 3.2 ns lifetime corresponds to the **AD3** alloxazinic monoanion. The neutral form is detectable up to pH = 11, while the alloxazinic monoanion exists in the 8 – 12 pH range. Comparing to 5-DAll, 9-methyl-5-deazaalloxazine has longer fluorescence lifetimes of the neutral and alloxazinic monoanionic forms: its neutral form lives 31 ns, while the alloxazinic monoanion lives 16 ns.<sup>18</sup>

The fluorescence emission at 460 and 500 nm has strong contributions of the isoalloxazinic monoanion and dianion of 5-DAll, with some contribution of the alloxazinic monoanion (see **Figure 11B**). We identify the longer-lived component with about 11.7 ns lifetime as the **ID1** isoalloxazinic monoanion. The fluorescence decays at pH 13 – 14 were mono-exponential at 500 nm; we identify the species with about 6.4 ns lifetime as the **ID13** dianion of 5-DAll. The tendency is opposite to what is observed in 9-methyl-5-dezaalloxazine, where the monoanion has the lifetime shorter (7.8 ns) than that of the respective dianion (9.2 ns).<sup>18</sup>

**Figure 12** shows the lifetimes of the emissive species of 1,3Me-5-DAll in function of pH. In acidic conditions we observe very short-lived (about 11 ps) fluorescence decay, probably from the **CMe5D<sup>+</sup>** alloxazinic cation.

Insert Figure 12

Additionally, the **NMe5D** neutral form is emitting in acidic, neutral, and basic conditions. Its lifetime is about 5.2 ns in neutral and basic pH, becoming shorter in acidic conditions due to quenching by protons.

The mechanism of fluorescence quenching is quite complex in this case, probably due to ground-state complexation by the **NMe5D** neutral form. The results of the kinetic study of fluorescence quenching of the **NMe5D** neutral form in function of  $H^+$  concentration are shown in **Figure 3s** in the Supporting Information. The obtained Stern-Volmer constant from the time – resolved experiments is  $K_{SV4} = 0.82 \pm 0.07$ . The value of the respective quenching rate constant is  $k_q = (2.28 \pm 0.13) \times 10^8 \text{ s}^{-1}$ . The ratios of the fluorescence intensities ( $I_0/I$ ) grow quickly with the growing proton concentration and the plot of  $I_0/I$  vs.  $[H^+]$  is apparently nonlinear. We believe this is due mostly to the increasing of concentration of the neutral form in the mixture both in the ground and in the excited state.

## Conclusions

The fluorescent species of 5-DAll and 1,3Me-5-DAll, existing in aqueous solutions at different pH, were studied using steady-state and time-resolved methods.

The 5-DAll cation, with the proton located at the N(10) position of the molecule, has an alloxazinic form in the ground state and an isoalloxazinic form in the excited state. The emission of this isoalloxazinic cation and its lifetime were probed for the first time. It exists in the solutions up to about  $pH \approx 1$ . In addition, this cation is quenched by protons in a dynamic process.

The 1,3Me-5-DAll cation has alloxazinic form in the ground state and no detectable fluorescence. Similarly, 10-ethyl-5-deaza*iso*alloxazine, studied by us earlier, has cation that reveals no fluorescence. Additionally, we can conclude that cations of 5-DAll, 1,3Me-5-DAll and even cation of 10-ethyl-5-deaza*iso*alloxazine, have alloxazinic forms in their ground

states. The neutral forms of 5-DAll and 1,3Me-5-DAll are also quenched in acidic conditions, but these processes for both compounds are both static and dynamic.

Contrary to that, as we studied previously, the cation of 9-methyl-5-deazaalloxazine is not detectable at  $\text{pH} < 2$  and its neutral form is not quenched in acidic conditions.

The  $\text{p}K_{\text{a}}$  values reflecting the acid-base equilibria between the neutral form of 5-DAll and its two anionic forms are the same in the ground state, and the  $\text{p}K_{\text{a}}^*$  values reflecting the acid-base equilibria between neutral and anionic forms of 5-DAll in the excited state is also similar. The  $\text{p}K_{\text{a}}$  and  $\text{p}K_{\text{a}}^*$  values for the formation of the dianion of 5-DAll from the two monoanions are quite similar.

Additionally, we used synchronous fluorescence spectroscopy and three-dimensional spectroscopy to show that these techniques are very useful during studies of spectral and photophysical properties of 5-DAll and 1,3Me-5-DAll in the wide range of pH values.

## Acknowledgments

This study was supported by the research grant DEC-2012/05/B/ST4/01207 from The National Science Centre of Poland (NCN).

## References

1. P. Hemmerich, V. Massey and H. Fenner, *FEBS Lett.*, 1977, **84**, 5–21 and reference cited therein.
2. L. D. Eirich, G. D. Vogels and R. S. Wolfe, *Biochem.*, 1978, **17**, 4583–4593.
3. F. Yoneda and K. Tanaka, *Med. Res. Rev.*, 1987, **7**, 77–506 and references cited therein.
4. V. Nadaraj, S. T. Selvi, S. Mohan and T. D. Thangadurai, *Med. Chem. Res.*, 2012, **21**, 2911–2919.
5. H. I. Ali, N. Ashida and T. Nagamatsu, *Bioorg. Med. Chem.*, 2008, **16**, 922–940.
6. Y. Ikeuchi, M. Sumiya, T. Kawamoto, N. Akimoto, Y. Mikata, M. Kishigami, S. Yano, T. Sasaki and F. Yoneda, *Bioorg. Med. Chem.*, 2000, **8**, 2027–2035.
7. Y. Kanaoka, Y. Ikeuchi, T. Kawamoto, K. Bessho, N. Akimoto, Y. Mikata, M. Nishida, S. Yano, T. Sasaki and F. Yoneda, *Bioorg. Med. Chem.*, 1998, **6**, 301–314.
8. T. Kawamoto, Y. Ikeuchi, J. Hiraki, Y. Eikyu, K. Shimizu, M. Tomishima, K. Bessho, F. Yoneda, Y. Mikata, M. Nishida, K. Ikehara and T. Sasaki, *Bioorg. Med. Chem. Lett.*, 1995, **5**, 2109–2114.
9. J. M. Wilson, G. Henderson, F. Black, A. Sutherland, R. L. Ludwig, K. H. Vousden and D. J. Robins, *Bioorg. Med. Chem.*, 2007, **15**, 77–86.
10. K. Nahm, W. S. Kim and K. Y. Moon, *Bioorg. Med. Chem. Lett.*, 1993, **3**, 2631–2634.
11. A. Koziółowa, N. V. Visser, J. Koziół and M. M. Szafran, *J. Photochem. Photobiol. A*, 1996, **93**, 157–163.
12. D. Prukała, I. Khmelinskii, J. Koput, M. Gierszewski, T. Pędziński and M. Sikorski, *Photochem. Photobiol.* **2014**, **90**, 972–988.
13. Koziół, J. *Photochem. Photobiol.*, 1969, **9**, 45–53.
14. P. S. Song, M. Sun, A. Koziółowa and J. Koziół, *J. Am. Chem. Soc.*, 1974, **96**, 4319–4323.
15. E. Sikorska, I. Khmelinskii, W. Prukała, S. L. Williams, M. Patel, D. R. Worrall, J. L. Bourdelande, J. Koput and M. Sikorski, *J. Phys. Chem. A*, 2004, **108**, 1501–1508.
16. S. T. Kim, P. F. Heelis and A. Sancar, *Biochem.*, 1992, **31**, 11244–11248.
17. D. Prukała, E. Sikorska, J. Koput, I. Khmelinskii, J. Karolczak, M. Gierszewski, and M. Sikorski, *J. Phys. Chem. A*, 2012, **116**, 7474–90.
18. D. Prukała, M. Gierszewski, T. Pędziński and M. Sikorski, *J. Photochem. Photobiol. A*, 2014, **275**, 12–20.
19. N. Lasser and J. Feitelson, *Photochem. Photobiol.*, 1977, **25**, 451–456.
20. A. Koziółowa, *Photochem. Photobiol.*, 1979, **29**, 459–471.

- 564 21. A. Tyagi and A. Penzkofer, *Photochem. Photobiol.*, 2011, **87**, 524-533.
- 565 22. J. Karolczak, D. Komar, J. Kubicki, T. Wrozowa, K. Dobek, B. Ciesielska and A.
- 566 Maciejewski, *Chem. Phys. Lett.*, 2001, **344**, 154-164.
- 567 23. DATAN 3.1, ISS Inc. USA, 2012, <http://www.iss.com/fluorescence/software/datan.html>
- 568 24. Y-O. Li, X-Y. Li, A. A. F. Shindi, Z-X. Zou, Q. Liu, L-R. Lin and N. Li, *Rev. Fluor.*,
- 569 2012, **2010**, 95-117.
- 570 25. T. Vodingh, *Anal. Chem.*, 1978, **50**, 396-401.

571  
572



573 **Caption for Table:**

574 **Table 1.** Molar absorption coefficients and quantum yields of ionic and neutral forms of 5-

575 DAll and 1,3Me-5-DAll.

576

**Captions for Figures:**

**Figure 1.** Structures and atom numbering of the studied compounds, and the structure of the simple alloxazine for comparison.

**Figure 2.** The spectra of 5-DAll (left panels) and 1,3Me-5-DAll (right panels) in acidic conditions. The absorption spectra of (A) 5-DAll, and (B) 1,3Me-5-DAll. The emission spectra of (C) 5-DAll, and (D); 1,3Me-5-DAll. The fluorescence excitation spectra of (E) 5-DAll observed at  $\lambda = 460$  nm, and (F) 1,3Me-5-DAll observed at  $\lambda = 460$  nm.

**Figure 3.** Acid-base equilibria of 5-DAll and of 1,3Me-5-DAll in acidic conditions.

**Figure 4.** (A) - Absorption spectra of 5-DAll; (B) - Emission spectra of 5-DAll; (C) - Fluorescence excitation spectra observed at 420 nm; (D) - Fluorescence excitation spectra observed at 460 nm and 500 nm.

**Figure 5.** Acid-base equilibria of 5-DAll in basic conditions.

**Figure 6.** (A) - Absorption spectra of 5-DAll in 11.3 – 13.6 pH range; (B) - Emission spectra of 5-DAll in 11.6 – 13.3 pH; (C) - Fluorescence excitation spectra of 5-DAll registered at 420 nm; (D) - Fluorescence excitation spectra of 5DAll registered at 500 nm.

**Figure 7.** (A) - Raw synchronous fluorescence spectra of 5-DAll in acidic conditions with  $\Delta\lambda = 20$  nm; Raw SFS of 5-DAll with  $\Delta\lambda = 60$  nm; (B) - in acidic conditions; (C) - in 7.24 – 11.27 pH range; (D) - in 11.62 – 13.57 pH range.

**Figure 8.** Raw synchronous fluorescence spectra of 1,3Me-5-DAll from acidic conditions to pH = 10.95 with  $\Delta\lambda = 20$  nm.

**Figure 9.** (A) - Total fluorescence spectra of 5-DAll at pH -0.48; (B) - Contour map of total fluorescence of 5-DAll; at pH -0.48; (C) - at pH 4.80; (D) - at pH 9.05; (E) - at pH 11.62; (F) - at pH 12.51; (G) - at pH 13.57 (G); (G) - Total fluorescence spectra of 5-DAll pH 13.57.

**Figure 10.** (A) - Plot of the lifetimes of 5-DAll vs.  $-\log [H^+]$  using  $\lambda_{exc} = 375$  nm and  $\lambda_{em} = 420$  nm and  $\lambda_{exc} = 338$  nm and  $\lambda_{em} = 420$  nm; (B) - Plot of the lifetimes of 5-DAll vs.  $-\log [H^+]$  using  $\lambda_{exc} = 375$  nm and  $\lambda_{em} = 500$  nm.

**Figure 11.** (A) - Plots of fluorescence lifetimes of fluorescent species of 5-DAll vs. pH (2 – 14). Samples excited at  $\lambda = 368$  nm and observed at  $\lambda = 420$  nm; (B) - samples excited at  $\lambda = 368$  nm and observed at  $\lambda = 460$  nm and  $\lambda = 500$  nm (B).

**Figure 12.** Plots of the fluorescence lifetimes of the fluorescent species of 1,3Me-5-DAll vs.  $-\log [H^+]$ . Samples excited at  $\lambda = 368$  nm and  $\lambda = 375$  nm, and observed at  $\lambda = 430$  nm and at  $\lambda = 460$  nm.

**Table 1.** Molar absorption coefficients and quantum yields of ionic and neutral forms of 5-DAll and 1,3Me-5-DAll.

Compound (Form)	$-\log [\text{H}^+]$	$\varepsilon / \text{dm}^3 \text{mol}^{-1} \text{cm}^{-1}$ $\lambda^{\text{a}} / \text{nm}$	Quantum yield ( $\phi$ ) $\lambda^{\text{b}}_{\text{exc}} / \text{nm}$
5-DAll			
C5D <sup>+</sup>	−0.48	14400 (331)	0.02 (320)
C5D <sup>+</sup> + N5D	0.30	-	0.07 (320)
N5D	1.10	4300 (354)	0.11 (320)
	2.5		0.18 (320)
	7.24	8500 (312)	0.21 (320)
AD3 + ID1		-	0.07 (320)
AD3	10.16	8600 (358)	-
ID1		3900 (380)	0.16 (410)
ID13	13.57	5400 (391)	0.19 (320)
			0.19 (410)
1,3Me-5-DAll			
CMe5D <sup>+</sup>	-0.43	7800 (332)	-
NMe5D			0.002 (320)
NMe5D	0.3		0.08 (320)
NMe5D	1.54	3600 (357)	0.17 (320)
NMe5D	3.14	6500 (312)	0.19 (320)
NMe5D	7.18		0.19 (320)
NMe5D	10.95		0.20 (320)

<sup>a</sup> – The wavelengths for which the molar absorption coefficients were determined ( $\lambda_{\text{max}}$ ).

<sup>b</sup> – Excitation wavelengths used for collection of fluorescence of appropriate forms of 5-DAll and 1,3Me-5-DAll used for quantum yield calculation.

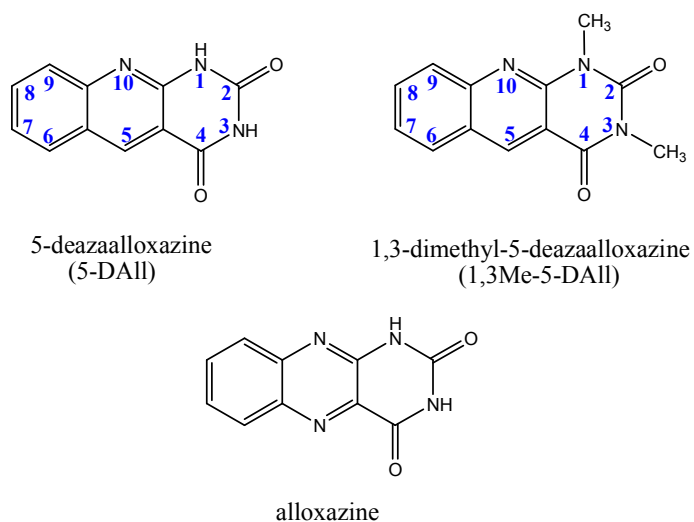


**Figure 1.** Structures and atom numbering of the studied compounds, and the structure of the simple alloxazine for comparison.

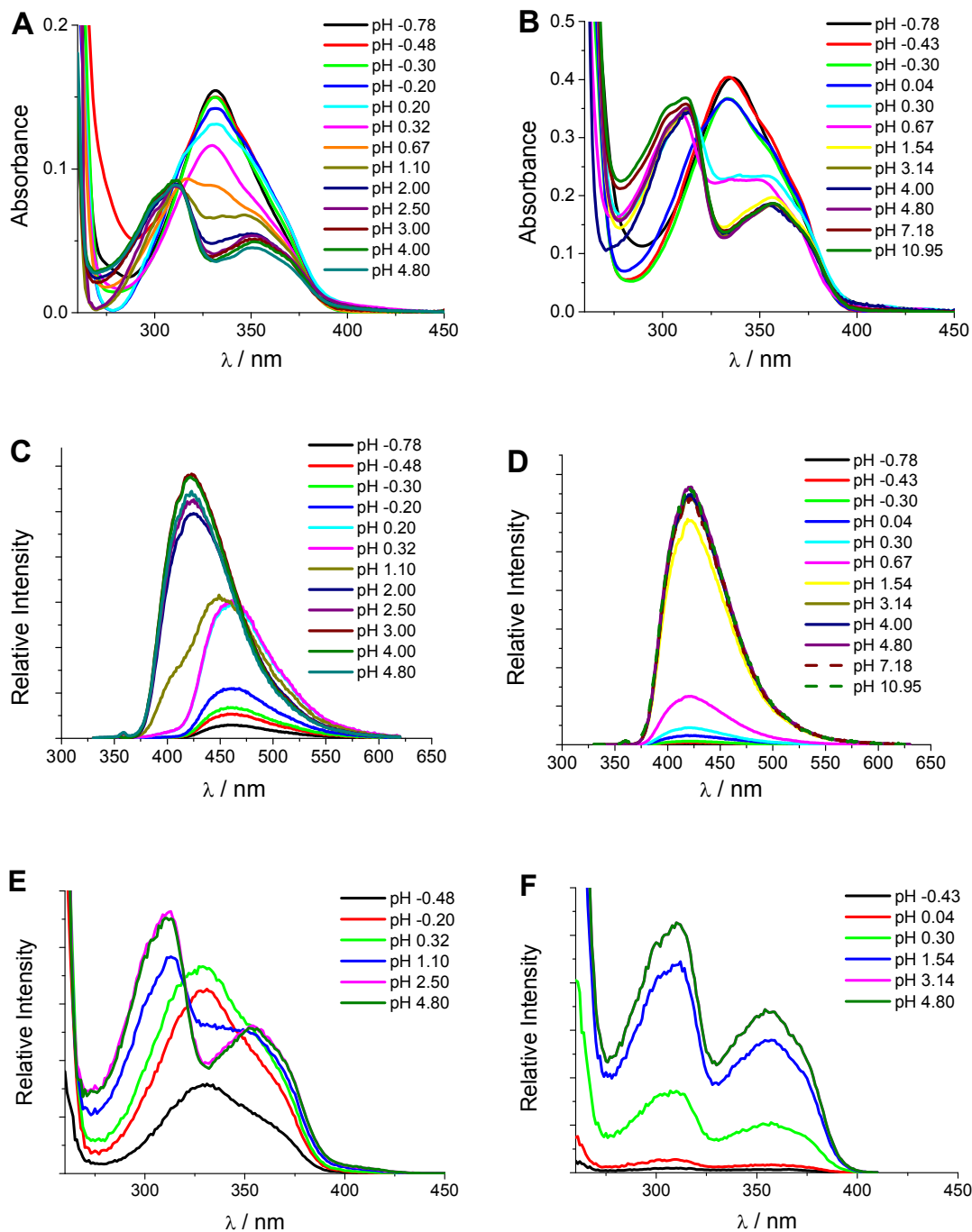


**Figure 2.** The spectra of 5-DAll (left panels) and 1,3Me-5-DAll (right panels) in acidic conditions. The absorption spectra of (A) 5-DAll, and (B) 1,3Me-5-DAll. The emission spectra of (C) 5-DAll, and (D); 1,3Me-5-DAll. The fluorescence excitation spectra of (E) 5-DAll observed at  $\lambda = 460$  nm, and (F) 1,3Me-5-DAll observed at  $\lambda = 460$  nm.

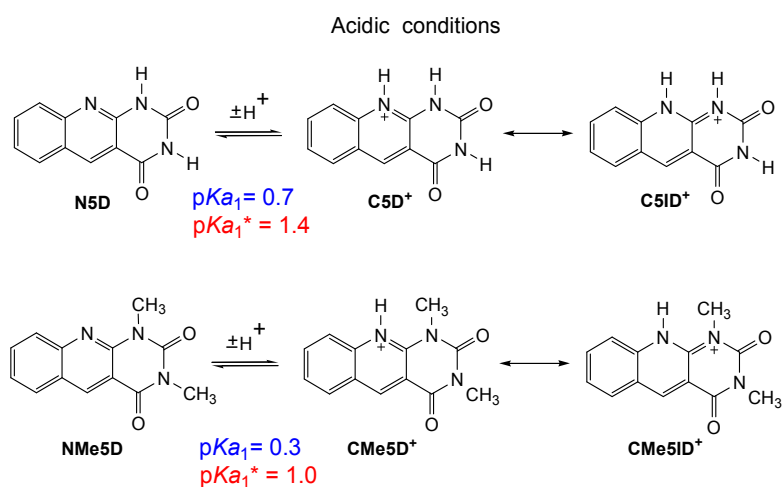


**Figure 3.** Acid-base equilibria of 5-DAll and of 1,3Me-5-DAll in acidic conditions.

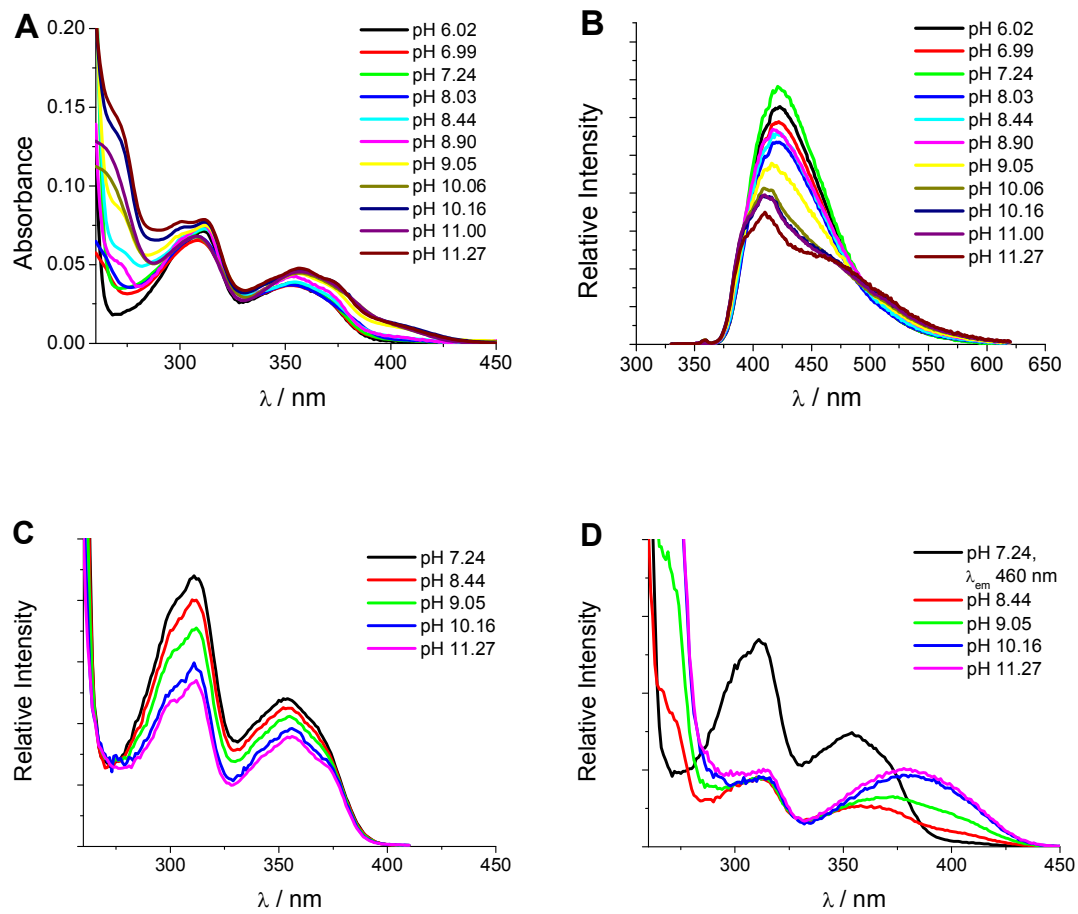


**Figure 4.** (A) - Absorption spectra of 5-DAll; (B) - Emission spectra of 5-DAll; (C) - Fluorescence excitation spectra observed at 420 nm; (D) - Fluorescence excitation spectra observed at 460 nm and 500 nm.



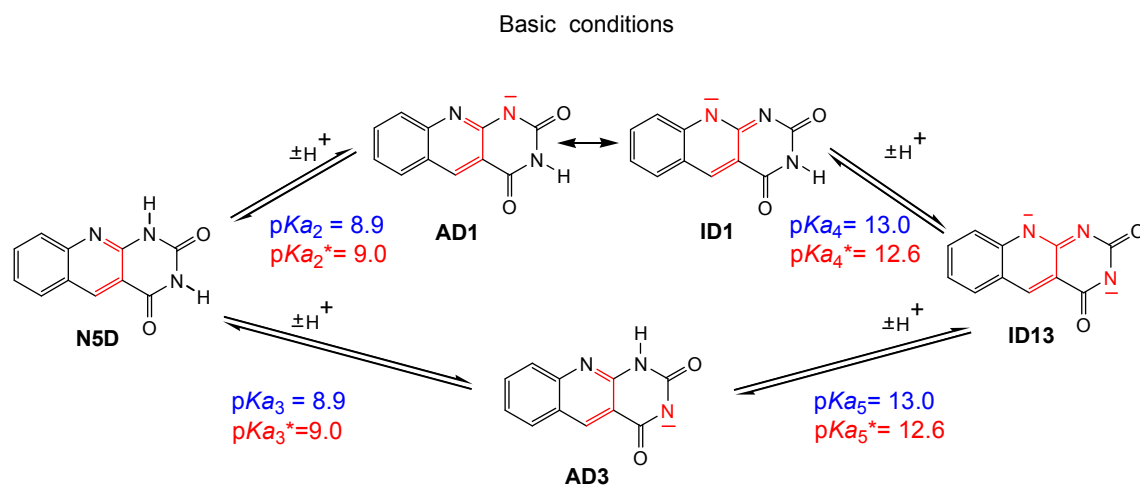


**Figure 5.** Acid-base equilibria of 5-DAll in basic conditions.

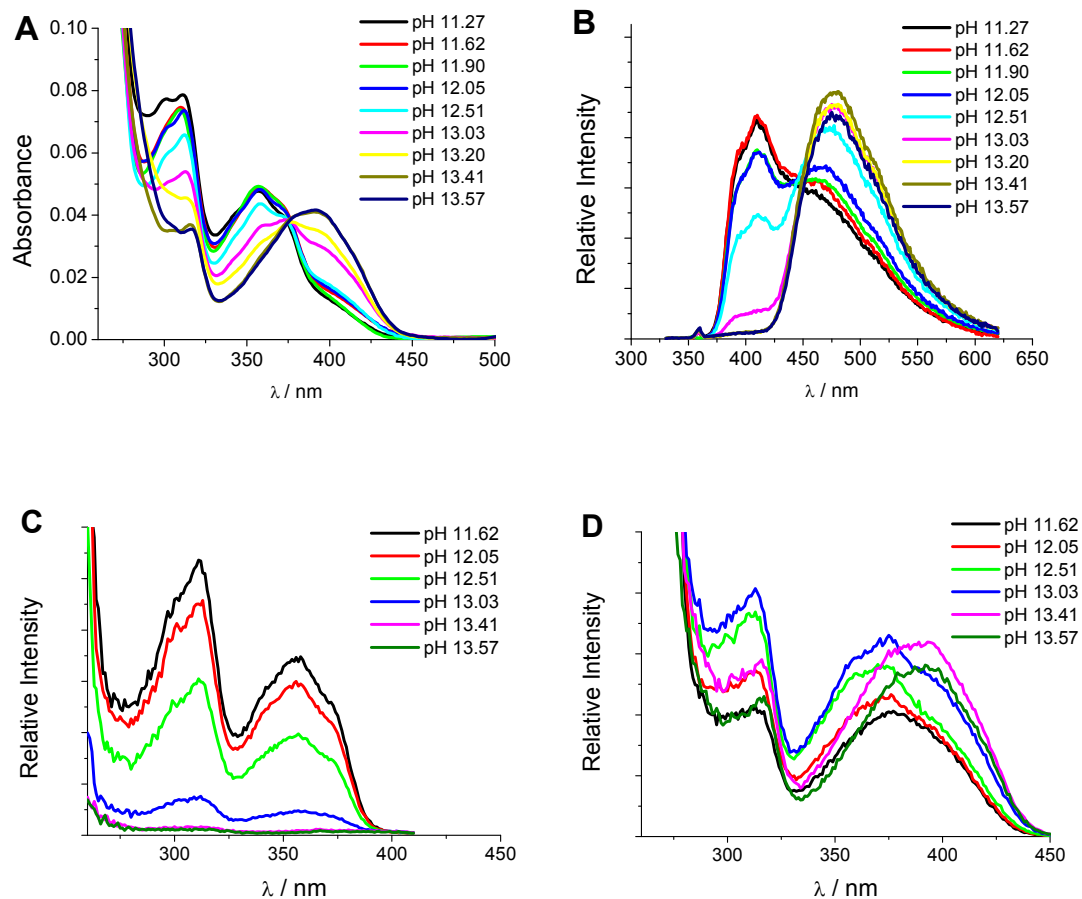


**Figure 6.** (A) - Absorption spectra of 5-DAll in 11.3 – 13.6 pH range; (B) - Emission spectra of 5-DAll in 11.6 – 13.3 pH; (C) - Fluorescence excitation spectra of 5-DAll registered at 420 nm; (D) - Fluorescence excitation spectra of 5DAll registered at 500 nm.

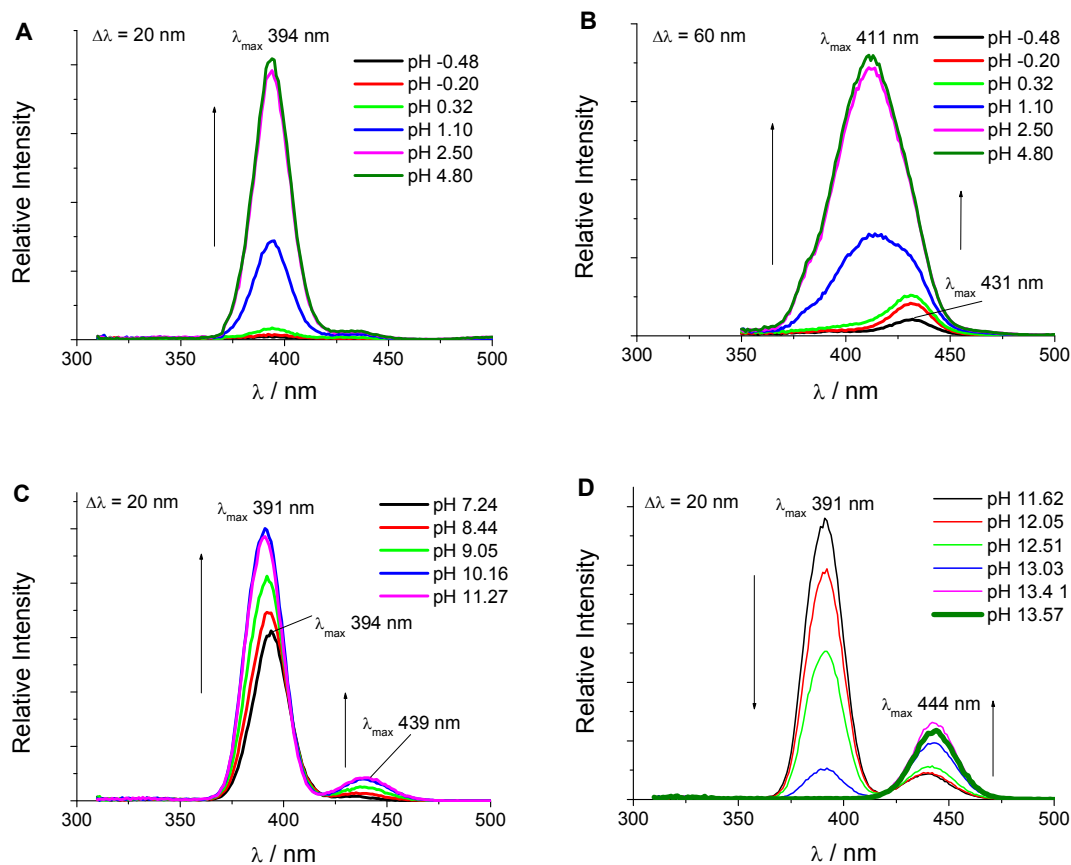


**Figure 7.** (A) - Raw synchronous fluorescence spectra of 5-DAll in acidic conditions with  $\Delta\lambda = 20$  nm; Raw SFS of 5-DAll with  $\Delta\lambda = 60$  nm; (B) - in acidic conditions; (C) - in 7.24 – 11.27 pH range; (D) - in 11.62 – 13.57 pH range.

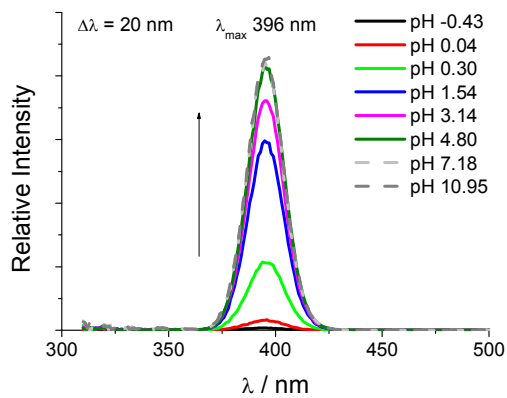


**Figure 8.** Raw synchronous fluorescence spectra of 1,3Me-5-DAlI from acidic conditions to pH = 10.95 with  $\Delta\lambda = 20$  nm.

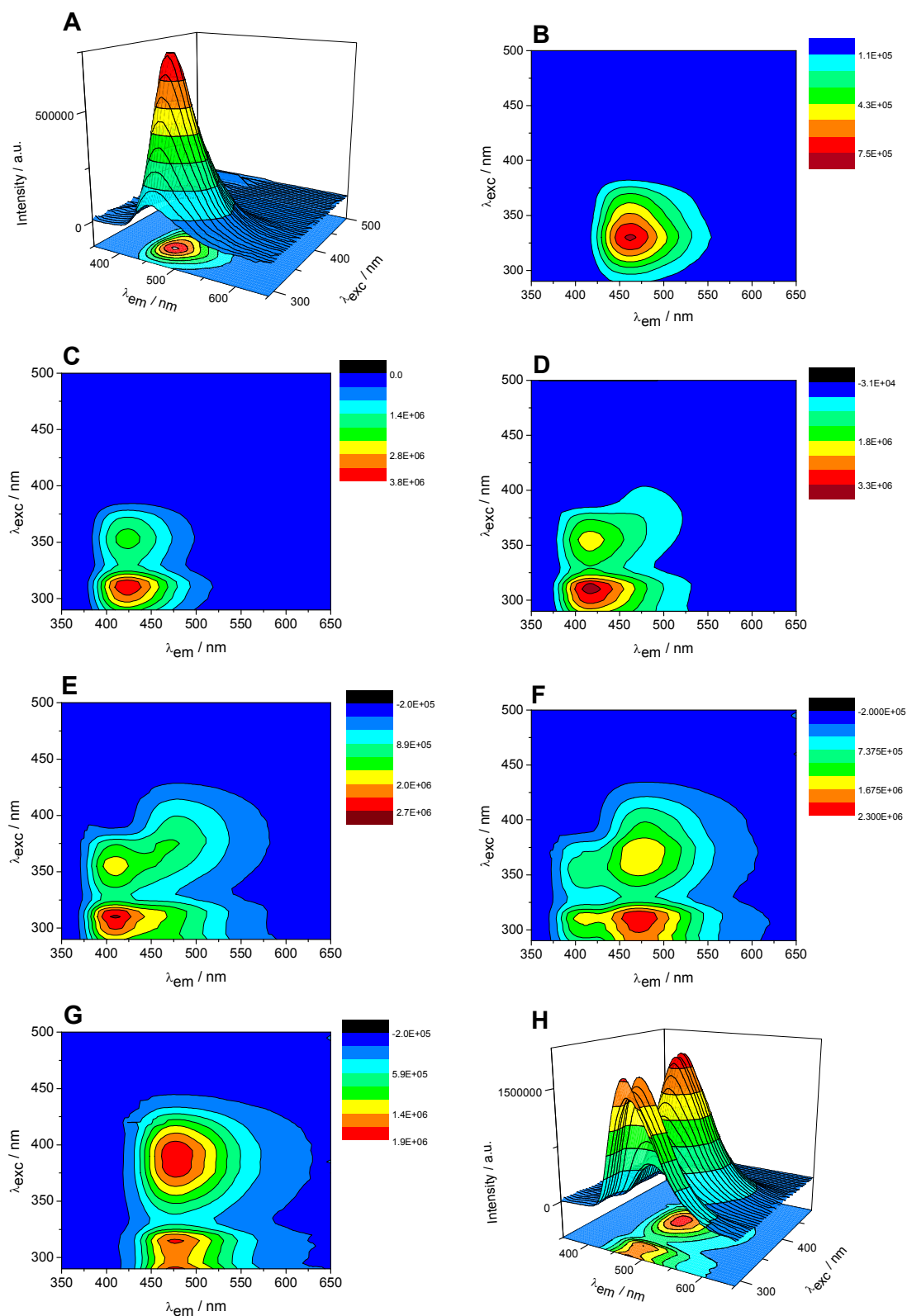


**Figure 9.** (A) - Total fluorescence spectra of 5-DAll at pH -0.48; (B) - Contour map of total fluorescence of 5-DAll; at pH -0.48; (C) - at pH 4.80; (D) - at pH 9.05; (E) - at pH 11.62; (F) - at pH 12.51; (G) - at pH 13.57 (G); (G) - Total fluorescence spectra of 5-DAll pH 13.57.

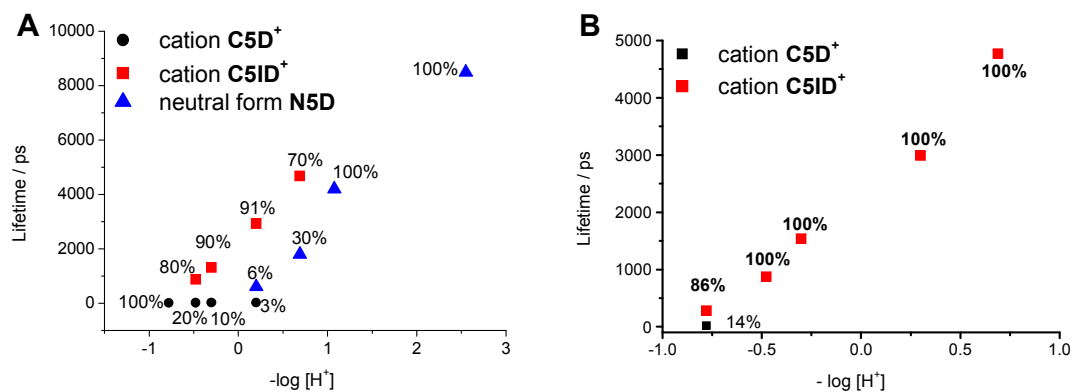


**Figure 10.** (A) - Plot of the lifetimes of 5-DAll vs.  $-\log [\text{H}^+]$  using  $\lambda_{\text{exc}} = 375 \text{ nm}$  and  $\lambda_{\text{em}} = 420 \text{ nm}$  and  $\lambda_{\text{exc}} = 338 \text{ nm}$  and  $\lambda_{\text{em}} = 420 \text{ nm}$ ; (B) - Plot of the lifetimes of 5-DAll vs.  $-\log [\text{H}^+]$  using  $\lambda_{\text{exc}} = 375 \text{ nm}$  and  $\lambda_{\text{em}} = 500 \text{ nm}$ .

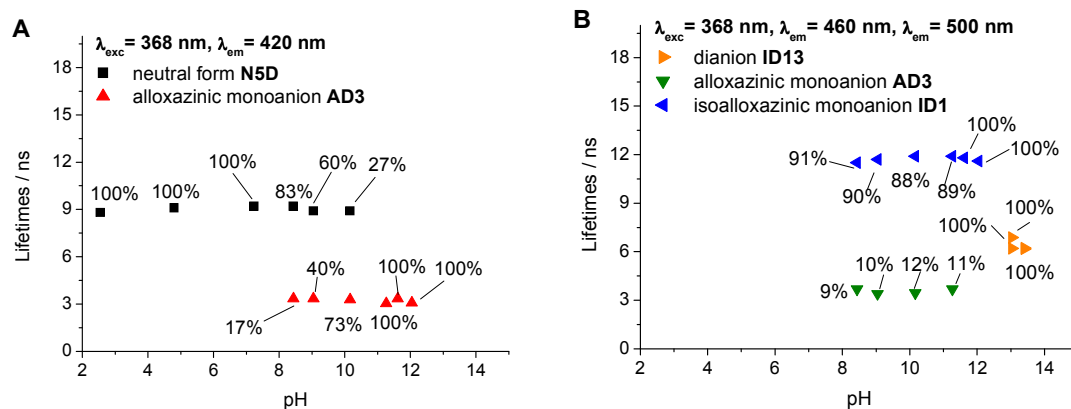


**Figure 11.** (A) - Plots of fluorescence lifetimes of fluorescent species of 5-DAll vs. pH (2 – 14). Samples excited at  $\lambda = 368 \text{ nm}$  and observed at  $\lambda = 420 \text{ nm}$ ; (B) - samples excited at  $\lambda = 368 \text{ nm}$  and observed at  $\lambda = 460 \text{ nm}$  and  $\lambda = 500 \text{ nm}$  (B).

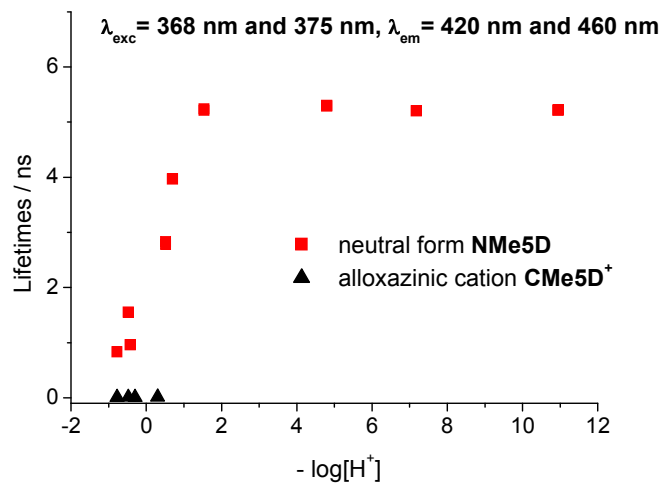


**Figure 12.** Plots of the fluorescence lifetimes of the fluorescent species of 1,3Me-5-DAll vs.  $-\log [H^+]$ . Samples excited at  $\lambda = 368 \text{ nm}$  and  $\lambda = 375 \text{ nm}$ , and observed at  $\lambda = 430 \text{ nm}$  and at  $\lambda = 460 \text{ nm}$ .